Solid helium. I. Ground-state energy calculated by a lowest-order constrained-variation method

Otto Svorstøl and Erlend Østgaard
Fysisk Institutt, Allmennvitenskapelige Høgskole, Universitetet i Trondheim, N-7055 Dragvoll, Norway
(Received 7 March 1986)

The ground-state energy of solid helium is calculated by means of a modified variational lowest-order constrained-variation (LOCV) method. Both ^{3}He and ^{4}He in the bcc, fcc, and hcp structures, as well as two possible spin configurations for ^{3}He, are considered, and the calculations are done for five different two-body potentials. Theoretical results for the ground-state energy per particle are -0.3 to $+$ 1.8 K for solid ^{3}He at a particle density of $0.42\sigma^{-3}$ or a molar volume of 24 cm^3/mol, and -6.1 to -3.2 K for solid ^{4}He at a particle density of $0.50\sigma^{-3}$ or a molar volume of 20 cm^3/mol, where $\sigma=2.556$ Å. The corresponding experimental results are -1.0 and -5.6 K, respectively. For higher densities, our theoretical results are in even better agreement with experimental results.

I. INTRODUCTION

Solid ^{3}He and ^{4}He are of interest as quantum solids, but quantum crystals such as helium cannot be treated by the classical theory of lattice dynamics.[1] The two-body potential has a very strong repulsion at small distances, which produces strong short-range correlations and a relatively large zero-point motion because of the small atomic mass and the relatively weak attractive part of the interaction. The zero-point energy is comparable to the potential energy, and the root-mean-square deviation of an atom from its equilibrium position at a lattice site is not small compared with the nearest-neighbor distance or the lattice constant. Anharmonic effects are important, even at zero temperature, and not only does the usual theory of lattice dynamics converge poorly, but the harmonic approximation simply breaks down.

Some early attempts[2,3] to study quantum crystals were made by anharmonic theory, and calculations were in fair agreement with experimental results. Many approximations were used, however, making the results unreliable. Bernardes and Primakoff[4,5] then made the first attempt to include correlations in a partly variational, partly phenomenological calculation of the ground-state energy of solid ^{3}He, using spherically symmetric Gaussian single-particle wave functions. They replaced the true interaction by a one-parameter effective interaction at small distances by introducing a cutoff in the potential to avoid the singularity problem when the relative interparticle distance $r\rightarrow 0$. The cutoff parameter was determined phenomenologically by fitting the ground-state energy and the root-mean-square deviation of the atoms from their lattice sites for solid ^{4}He. Bernardes and Primakoff, however, underestimated the kinetic energy, overestimated the exchange integral, and found a rather large root-mean-square deviation.

Saunders[6] then calculated properties of solid ^{3}He, using Jastrow-type[7] wave functions and including correlation effects and the lattice symmetry. He derived an approximate differential equation for the correlation function, but a single-particle function could be shown to diverge and the equation for the correlation function was solved incorrectly. Saunders's approach was analyzed by Garwin and Landesman,[8] who made some improvements. They found, however, that his approach breaks down completely for ^{4}He. The usual approach for solid helium has later been to apply variational methods, assuming that we can make cluster expansions as suggested by Van Kampen,[9] using a trial ground-state wave function containing short-range Jastrow correlations.

The methods of Nosanow *et al.*[10–13] and Brueckner *et al.*[14,15] were then based on an approximate expression for the energy expectation value obtained by a cluster expansion which had to be truncated and then varied to give an estimate of the ground-state energy. A localized wave function, i.e., a product of short-range two-particle correlation functions and Gaussian single-particle functions centered about the lattice sites, was used. The cluster expansion of Nosanow is grouped in terms of increasing numbers of intercorrelated particles, i.e., he proceeds from one term to the next by adding a particle at a time and the derivation is given for a general wave function. The expansion of Brueckner and Frohberg[14] was ordered by increasing the number of factors of the correlation function, i.e., they assume the Jastrow function from the beginning and derive an expansion whose successive terms differ by the inclusion of a single additional correlation factor. The relationship between the two expansions has been studied by Trickey.[16] Starting with Gaussian Jastrow trial wave functions, Massey and Woo[17,18] also made calculations where they reordered the Nosanow expansion so that particles outside the cluster had the particle correlations of the liquid.

Most of the theoretical work on the ground-state energy of solid helium has been variational calculations, using a correlated trial wave function. Iwamoto and Namaizawa,[18] Brandow,[20] and Østgaard,[21] however, used self-consistent methods similar to the reaction-matrix Breuckner theory[22] for nuclear-matter calculations, which produced an integrodifferential equation, similar to the Bethe-Goldstone equation,[23] to be solved to give the effective interaction or reaction-matrix elements. But the ac-

curacy of their methods is not known, so their agreement with experimental results may be a coincidence.

Guyer and Zane[24,25] and Glyde and Khanna[26] also proposed methods based on cluster expansions of the ground-state energy, using model Hamiltonians. They also derived a two-particle equation similar to the Bethe-Goldstone equation, and described the motion of a pair of particles in the average field produced by the remaining lattice. No self-consistency follows, however, from the Guyer theory. Also, Horner[27] and Ebner and Sung[28] have introduced a time-dependent formalism similar to the Brueckner theory but expressed by Green functions.

Finally, using wave functions with Gaussian single-particle functions in Monte Carlo calculations, Hansen *et al.*[29–31] and Ceperley *et al.*[32] have obtained lower ground-state energies in better agreement with experimental results for solid helium. We now want to calculate the ground-state energy, the pressure, and the compressibility of solid helium by means of a modified variational lowest-order constrained-variation (LOCV) method.[33,34]

II. THE CLUSTER EXPANSION

To obtain the equation of state for a system of N particles (in statistical mechanics) we generally expand the configuration integral Q_N as a series in the fugacity. Alternatively, Van Kampen[9] has given a cluster expansion for Q_N, where Q_N is represented by an infinite product instead of an infinite series (i.e., infinite in the sense $N\to\infty$). Nosanow[11] has used this idea to obtain a cluster expansion for the energy.

The energy for a system of particles is given by

$$E=\langle\Psi|H|\Psi\rangle/\langle\Psi|\Psi\rangle\ , \tag{2.1}$$

where H is the total Hamiltonian for the system and Ψ is the total wave function. Following the idea of Van Kampen, we can obtain the energy as

$$E=\sum_{n=1}^{N}E_n\ , \tag{2.2}$$

and this series will hopefully converge so fast that it is sufficient to keep only the first two terms when two-body correlations are the most important correlations in the system.

We define a wave function $\Psi_n(\{n\})$ and a Hamiltonian $H_n(\{n\})$ depending on the coordinates of a set of n particles, i.e., $\Psi_1(\{1\})$ is a single-particle wave function, and $\Psi_2(\{2\})$ is a two-particle wave function. The Hamiltonian is

$$H(\{n\})=-(\hbar^2/2m)\sum_{i=1}^{n}\nabla_i^2+\sum_{\substack{i,j=1\\ i\neq j}}^{n}V_{ij}\ , \tag{2.3}$$

where V_{ij} is a two-body potential.

Since we are going to keep only one-body and two-body terms, we truncate the expansion (2.2) and calculate E from

$$\begin{aligned}E_1&=\sum_{i=1}^{N}\langle\Psi_1(\mathbf{r}_i)|H_1(\mathbf{r}_i)|\Psi_1(\mathbf{r}_i)\rangle/\langle\Psi_1(\mathbf{r}_i)|\Psi_1(\mathbf{r}_i)\rangle\\&=\sum_{i=1}^{N}C_1(i)\ ,\end{aligned} \tag{2.4}$$

and

$$\begin{aligned}E_2&=\sum_{1\le i<j\le N}\sum\langle\Psi_2(\mathbf{r}_i,\mathbf{r}_j)|H_2(\mathbf{r}_i,\mathbf{r}_j)|\Psi_2(\mathbf{r}_i,\mathbf{r}_j)\rangle/\langle\Psi_2(\mathbf{r}_i,\mathbf{r}_j)|\Psi_2(\mathbf{r}_i,\mathbf{r}_j)\rangle-C_1(i)-C_1(j)\\&=\tfrac{1}{2}\sum_{i,j=1}^{N}C_2(ij)\ ,\end{aligned} \tag{2.5}$$

where the factor $\frac{1}{2}$ prevents double counting. The cluster expansion for the energy is then

$$E=\sum_{i=1}^{N}C_1(i)+\tfrac{1}{2}\sum_{i,j=1}^{N}C_2(ij)+\cdots\ , \tag{2.6}$$

where the ellipsis represents higher-order terms, and these expressions are the basis for (both liquid and solid phase) many-body LOCV calculations.

III. GENERAL THEORY

Equation (2.6) is the basis for a method of lowest-order constrained variation (LOCV) suggested by Pandharipande,[35,36] and the LOCV method applied to a liquid phase has been treated and explained elsewhere.[37,38] If we assume that the interactions in the system are mainly two-body interactions between pairs of particles, we may in general approximate the many-body wave function $\Psi(1,2,\ldots,N)$ by a Jastrow function:

$$\Psi=\prod_{i(<j)}\left[\sum_l f_l(r)\hat{P}^l\right]\hat{A}\prod_i\phi_i(\mathbf{r})\ , \tag{3.1}$$

where we choose the correlation function

$$f(r)=\sum_l f_l(r)\hat{P}^l \tag{3.2}$$

in a variational calculation to minimize the two-particle contribution to the energy. Here, r is the relative distance between the interacting particles, l is the orbital angular momentum quantum number of the correlated pair ij, $\hat{P}^l$ is the projection operator for the lth partial wave, $\hat{A}$ is a symmetrization or antisymmetrization operator to ensure the proper wave function for bosons or fermions, and $\phi_i(\mathbf{r}_i)$ is the uncorrelated single-particle wave function.

Before evaluating the energy expression (2.6), however, we have to make some assumptions concerning the lattice structure in the solid phase, the single-particle wave functions, and the interparticle potential. We shall calculate the energy assuming a bcc, fcc, or hcp lattice. Both bcc and fcc structures are likely at high densities since they permit a close packing of particles. The hcp structure is similar to the fcc structure, and calculations seem to give approximately the same energies for hcp and fcc lattices.

The single-particle wave functions $\phi_m(\mathbf{r}_i)$ are taken to

be Gaussians centered around the lattice site m, i.e.,

$$\phi_m(\mathbf{r}_i)=(\nu/\pi)^{3/4}\exp[-\tfrac{1}{2}\nu(\mathbf{r}_i-\mathbf{R}_m)^2] , \tag{3.3}$$

where $\mathbf{r}_i$ is the distance and direction from an arbitrary origin to the particle i, $\mathbf{R}_m$ is the distance and direction from the origin to the lattice site m, ν is a variational parameter giving the amplitude and spread of the wave function, and the energy is to be minimized with respect to this parameter. We assume that the long-range correlations in such dense systems determine the single-particle wave functions completely and that there are no deformations in the crystal structure, i.e., we assume the same uncorrelated two-particle wave functions in all l and s states. No partial-wave expansion is then necessary and $C_2(ij)$ will be on the same form in all states.

From (3.3) we get the correct normalization, i.e.,

$$\langle\phi_m(\mathbf{r}_i)\,|\,\phi_m(\mathbf{r}_i)\rangle=\int d^3r\,|\,\phi_m(\mathbf{r}_i)\,|^2=1 , \tag{3.4}$$

and the uncorrelated two-particle wave function is

$$\phi_2(ij)=[\phi_m(\mathbf{r}_i)\phi_n(\mathbf{r}_j)+(-1)^s\phi_m(\mathbf{r}_j)\phi_n(\mathbf{r}_i)] , \tag{3.5}$$

if we let s be the quantum number for the total spin of two particles and M_s the projection of this spin.

We then introduce relative and center-of-mass coordinates, i.e.,

$$\begin{aligned}&\mathbf{r}=\mathbf{r}_i-\mathbf{r}_j ,\\ &\mathbf{R}=\tfrac{1}{2}(\mathbf{r}_i+\mathbf{r}_j) ,\\ &\mathbf{R}_{mn}=\mathbf{R}_m-\mathbf{R}_n ,\\ &\delta=\tfrac{1}{2}(\mathbf{R}_m+\mathbf{R}_n) ,\end{aligned} \tag{3.6}$$

where $r=|\,\mathbf{r}\,|$ is the relative distance between particle i and particle j, and $R_{mn}=|\,\mathbf{R}_{mn}\,|$ is the distance between lattice site m and lattice site n. The relation

$$\mathbf{R}_m=\langle\mathbf{r}_i\rangle \tag{3.7}$$

defines m.

Using (3.6) we get

$$\begin{aligned}\phi_m(\mathbf{r}_i)\phi_n(\mathbf{r}_j)&=(\nu/\pi)^{3/2}\exp[-\nu(\mathbf{R}-\delta)^2]\\ &\quad\times\exp[-\tfrac{1}{4}\nu(\mathbf{r}-\mathbf{R}_{mn})^2]\\ &=\Phi(\mathbf{R})\phi(\mathbf{r}) .\end{aligned} \tag{3.8}$$

The normalization is taken to be

$$\begin{aligned}&\langle\Phi(\mathbf{R})\,|\,\Phi(\mathbf{R})\rangle=1 ,\\ &\langle\phi(\mathbf{r})\,|\,\phi(\mathbf{r})\rangle=1 ,\end{aligned} \tag{3.9}$$

and hence

$$\begin{aligned}&\Phi(\mathbf{R})=(2\nu/\pi)^{3/4}\exp[-\nu(\mathbf{R}-\delta)^2] ,\\ &\phi(\mathbf{r})=(\nu/2\pi)^{3/4}\exp[-\tfrac{1}{4}\nu(\mathbf{r}-\mathbf{R}_{mn})^2] .\end{aligned} \tag{3.10}$$

We also obtain

$$\begin{aligned}\phi_m(\mathbf{r}_j)\phi_n(\mathbf{r}_i)&=(\nu/\pi)^{3/2}\exp[-\nu(\mathbf{R}-\delta)^2\\ &\quad-\tfrac{1}{4}\nu(-\mathbf{r}-\mathbf{R}_{mn})^2]\\ &=\Phi(\mathbf{R})\phi(-\mathbf{r}) ,\end{aligned} \tag{3.11}$$

where

$$\begin{aligned}\phi(-\mathbf{r})&=(\nu/2\pi)^{3/4}\exp[-\tfrac{1}{4}\nu(-\mathbf{r}-\mathbf{R}_{mn})^2]\\ &=(\nu/2\pi)\exp[-\tfrac{1}{4}\nu(\mathbf{r}+\mathbf{R}_{mn})^2] .\end{aligned} \tag{3.12}$$

From (3.5), (3.8), and (3.11) we get

$$\begin{aligned}\phi_2(ij)&=\Phi(\mathbf{R})\phi(\mathbf{r})+(-1)^s\Phi(\mathbf{R})\phi(-\mathbf{r})\\ &=\Phi(\mathbf{R})\phi_a(\mathbf{r}) ,\end{aligned} \tag{3.13}$$

where

$$\phi_a(\mathbf{r})=\phi(\mathbf{r})+(-1)^s\phi(-\mathbf{r}) . \tag{3.14}$$

The correlated two-body wave function is given by (3.1), i.e.,

$$\begin{aligned}&\Psi=\prod_{i(<j)}f_{mn}(\mathbf{r})\hat{A}\prod_i\phi_m(\mathbf{r}_i) ,\\ &\Psi_2(ij)=\Phi(\mathbf{R})f_{mn}(\mathbf{r})\phi_a(\mathbf{r}) .\end{aligned} \tag{3.15}$$

The expectation value $C_1(i)$ in (2.4) is determined by

$$\begin{aligned}&H_1(\mathbf{r}_i)=-(\hbar^2/2m)\nabla_i^2 ,\\ &C_1(i)=\langle\phi_m(r_i)\,|\,-(\hbar^2/2m)\nabla_i^2\,|\,\phi_m(r_i)\rangle=\tfrac{3}{4}(\hbar^2/m)\nu ,\end{aligned} \tag{3.16}$$

or

$$\begin{aligned}&C_i(i)=\tfrac{3}{4}\hbar\omega ,\\ &\omega=(\hbar/m)\nu .\end{aligned} \tag{3.17}$$

The two-body contribution (2.5) to the energy is given by

$$\begin{aligned}&H_2(\mathbf{r}_i,\mathbf{r}_j)=-(\hbar^2/m)(\nabla_i^2+\nabla_j^2)+V(\,|\,\mathbf{r}_i-\mathbf{r}_j\,|\,) ,\\ &C_2(ij)=\langle\Psi_2(ij)\,|\,H_2(ij)\,|\,\Psi_2(ij)\rangle\\ &\qquad\times\langle\Psi_2(ij)\,|\,\Psi_2(ij)\rangle^{-1}-C_1(i)-C_1(j) ,\end{aligned} \tag{3.18}$$

where $H_2(\mathbf{r}_i,\mathbf{r}_j)$ is defined by (2.3), and $\Psi_2(ij)$ may be written

$$\Psi_2(ij)=f_{mn}(r)[\phi_m(\mathbf{r}_i)\phi_n(\mathbf{r}_j)+(-1)^s\phi_m(\mathbf{r}_j)\phi_n(\mathbf{r}_i)] . \tag{3.19}$$

Transforming to center-of-mass and relative coordinates we finally obtain

$$C_2(ij)=-(\hbar^2/m)(I_1/I_2)-\tfrac{3}{4}\hbar\omega+(I_3/I_2) , \tag{3.20}$$

where

$$\begin{aligned}&I_1=\langle\phi_a(\mathbf{r})f(r)\,|\,f(r)\nabla^2\,|\,\phi(\mathbf{r})\rangle ,\\ &I_2=\langle\phi_a(\mathbf{r})\,|\,f(r)\,|\,f(r)\phi(\mathbf{r})\rangle ,\\ &I_3=\langle\,\phi_a(\mathbf{r})f(r)\,|\,V(r)f(r)\\ &\qquad-(\hbar^2/m)[\nabla^2f(r)+2\nabla f(r)\nabla]\,|\,\phi(\mathbf{r})\rangle .\end{aligned} \tag{3.21}$$

The two-body contribution to the energy now contains three integrals, I_1, I_2, and I_3. In the numerical calculations we want to include all terms, even when $C_2(ij)$ is dominated by I_3, i.e., by the potential $V(r)$. The boundary conditions for the correlation function $f(r)$ are

$$f(r \geq d)=1 ,$$
$$f(r=0)=0 , \tag{3.22}$$
$$f'(r=d)=0 ,$$

where the "healing" distance d is to be determined later.

If we choose an arbitrary particle i to be located at the lattice site m, the other particles will be grouped in "shells" as if particle i were at the center. A shell then corresponds to a set of particles having the same average distance from the lattice site m. For the bcc crystal we obtain a nearest-neighbor distance a as a function of the particle density ρ, i.e.,

$$a=(\tfrac{3}{2}\sqrt{3}/\rho)^{1/3} , \tag{3.23}$$

and for the fcc and the hcp crystal we get

$$a=(\sqrt{2}/\rho)^{1/3} , \tag{3.24}$$

where

$$\rho=\Omega_0/N_0 , \tag{3.25}$$

when Ω_0 is the molar volume and N_0 is Avogadro's number. The distances to the 12 nearest shells for bcc and fcc structures and to the 17 nearest shells for hcp structure are given in Table I in units of a. Energetically favorable symmetric spin configurations for solid ^{3}He are also indicated, i.e., the spin configuration in the kth shell is given relatively to the particle i. The arrow to the left symbolizes the z component of the spin of the particles in the kth shell. The symbol $\frac{1}{2}(\uparrow\uparrow+\uparrow\downarrow)$ means that one-half of the particles in this shell have the same z component as particle i, while the other half of the particles have a z component in the opposite direction.

IV. THE LOCV METHOD

The two-body energy contribution from the kth shell, $C_2^k(ij)$, is given by (3.22). It will be an average sum over s if we take spins into account, and it is dependent on R_{mn}, which is the distance to the kth shell, i.e.,

$$C_2^k(ij)=\sum_s C_2^s(ij) ,$$
$$C_2^s(ij)=-(\hbar^2/m)(I_1^s/I_2^s)-\tfrac{3}{4}\hbar\omega+(I_3^s/I_2^s) , \tag{4.1}$$

where $\sum_s$ is to be understood as an averaged sum over s for a given M_s value. The corresponding correlation function $f(r)$ is then determined by our LOCV method.

We want to minimize $C_2^s(ij)$ with respect to $f(r)$ and we then approximate $C_2^s(ij)$ by

$$C_2^s(ij)\approx I_3^2=\langle \phi_a(\mathbf{r})f(r) \mid V(r)f(r)-(\hbar^2/m)[\nabla^2 f(r)+2\nabla(r)\cdot\nabla] \mid \phi(\mathbf{r})\rangle . \tag{4.2}$$

I_3^s then depends upon the angle between $\mathbf{r}$ and $\mathbf{R}_{mn}$ through $\phi_a(\mathbf{r})$ and $\phi(\mathbf{r})$. The θ dependence in I_3 is integrated out since the interaction is spherical symmetric. Using the simplified notation

$$\cos\theta\rightarrow x ,$$
$$\hbar^2/m\rightarrow\beta , \tag{4.3}$$

we obtain

TABLE I. Number of particles (n_k) in the kth shell and the distance R_{mn} (a) to the different shells expressed by the nearest-neighbor distance a for bcc, fcc, and hcp crystal structures. Indicated are also symmetric spin configurations which should be energetically most favorable for solid ^{3}He.

	bcc			fcc			hcp	
k	R_{mn} (a)	n_k	Spin configuration	R_{mn} (a)	n_k	Spin configuration	R_{mn} (a)	n_k
1	1	8	$\uparrow\downarrow$	1	12	$\frac{1}{2}(\uparrow\uparrow+\uparrow\downarrow)$	1	12
2	$\sqrt{4/3}$	6	$\uparrow\uparrow$	$\sqrt{2}$	6	$\uparrow\downarrow$	$\sqrt{2}$	6
3	$\sqrt{8/3}$	12	$\uparrow\uparrow$	$\sqrt{3}$	24	$\frac{1}{2}(\uparrow\uparrow+\uparrow\downarrow)$	$\sqrt{8/3}$	2
4	$\sqrt{11/3}$	24	$\uparrow\downarrow$	2	12	$\uparrow\uparrow$	$\sqrt{3}$	18
5	2	8	$\uparrow\uparrow$	$\sqrt{5}$	24	$\frac{1}{2}(\uparrow\uparrow+\uparrow\downarrow)$	$\sqrt{11/3}$	12
6	$\sqrt{16/3}$	6	$\uparrow\uparrow$	$\sqrt{6}$	8	$\uparrow\downarrow$	2	6
7	$\sqrt{19/3}$	24	$\uparrow\downarrow$	$\sqrt{7}$	48	$\frac{1}{2}(\uparrow\uparrow+\uparrow\downarrow)$	$\sqrt{5}$	12
8	$\sqrt{20/3}$	24	$\uparrow\uparrow$	$\sqrt{8}$	6	$\uparrow\uparrow$	$\sqrt{17/3}$	12
9	$\sqrt{8}$	24	$\uparrow\uparrow$	3	36	$\frac{1}{2}(\uparrow\uparrow+\uparrow\downarrow)$	$\sqrt{6}$	6
10	3	32	$\uparrow\downarrow$	$\sqrt{10}$	24	$\uparrow\downarrow$	$\sqrt{19/3}$	6
11	$\sqrt{32/3}$	12	$\uparrow\uparrow$	$\sqrt{11}$	24	$\frac{1}{2}(\uparrow\uparrow+\uparrow\downarrow)$	$\sqrt{20/3}$	12
12	$\sqrt{35/3}$	48	$\uparrow\downarrow$	$\sqrt{12}$	24	$\uparrow\uparrow$	$\sqrt{7}$	24
13							$\sqrt{22/3}$	6
14							$\sqrt{25/3}$	12
15							3	12
16							$\sqrt{29/3}$	24
17							$\sqrt{10}$	12

$$I_3^s = 2\pi \int_0^\infty r^2 dr \int_{-1}^{1} dx [Vf^2 - \beta f f'' - (2\beta/r) f f' + \beta\nu(r - R_m x) f f'] \phi_a \phi$$
$$= E_D + (-1)^s E_E \ . \tag{4.4}$$

The direct term in I_3 then is

$$E_D = 4\pi(\nu/2\pi)^{3/2} \int_0^\infty dr (2\nu r R_{mn})^{-1} \times r^2 ([Vf^2 - \beta f f'' - (2\beta/r) f f'] \{\exp[-\tfrac{1}{2}\nu(r - R_{mn})^2] - \exp[-\tfrac{1}{2}\nu(r + R_{mn})^2]\} + 2\beta f f' \{ [(2r)^{-1} + \tfrac{1}{2}\nu(r - R_{mn})] \exp[-\tfrac{1}{2}\nu(r - R_{mn})^2] - [(2r)^{-1} + \tfrac{1}{2}\nu(r + R_{mn})] \exp[-\tfrac{1}{2}\nu(r + R_{mn})^2] \}) \ . \tag{4.5}$$

We introduce a new wave function $\Phi(r)$, defined by

$$\Phi(r) = (\nu/2\pi)^{3/4} (2\nu r R_{mn})^{-1/2} \{\exp[-\tfrac{1}{2}\nu(r - R_{mn})^2] - \exp[-\tfrac{1}{2}\nu(r + R_{mn})^2]\}^{1/2} \ , \tag{4.6}$$

and hence

$$E_D = \int d^3 r \{ Vf^2 - \beta f f'' - (2\beta/r) f f' - 2\beta [\ln\Phi(r)]' f f' \} \Phi^2(r) \ . \tag{4.7}$$

The exchange term in I_3^s is

$$E_E = (\nu/2\pi)^{3/2} \int d^3 r [Vf^2 - \beta f f'' - (2\beta/r) f f' + \beta\nu r f f'] \exp[-\tfrac{1}{2}\nu(r^2 + R_{mn}^2)] \ . \tag{4.8}$$

We define $\Phi^*(r)$ to satisfy the condition

$$\Phi^*(r)\Phi(r) = (\nu/2\pi)^{3/2} \exp[-\tfrac{1}{2}\nu(r^2 + R_{mn}^2)] \ , \tag{4.9}$$

and we introduce $\Phi_a(r)$ by

$$\Phi_a(r) = \Phi(r) + (-1)^s \Phi^*(r) \ . \tag{4.10}$$

Using (4.6) and (4.9) we find

$$\Phi^*(r) = (\nu/2\pi)^{3/2} \exp[-\tfrac{1}{2}\nu(r^2 + R_{mn}^2)] / \Phi(r) = [\nu r R_{mn} / \sinh(\nu r R_{mn})] \Phi(r) \ , \tag{4.11}$$

$$\Phi'(r)/\Phi(r) + \Phi^{*\prime}(r)/\Phi^*(r) = [\ln\Phi(r)]' + [\ln\Phi^*(r)]' = -\nu r \ ,$$

and hence

$$E_E = \int d^3 r \{ Vf^2 - \beta f f'' - (2\beta/r) - \beta [\Phi'(r)/\Phi(r) + \Phi^{*\prime}(r)/\Phi^*(r)] f f' \} \times \Phi(r)\Phi^*(r) \ . \tag{4.12}$$

Our expression for I_3^s may be written

$$I_3^2 = \int d^3 r (Vf^2 - \beta f f'' - (2\beta/r) f f' - \beta \{ [\ln\Phi_a(r)]' + [\ln\Phi(r)]' \} f f') \times \Phi_a(r)\Phi(r) = \langle \Phi_a(r) \mid V_{\text{eff}} \mid \Phi(r) \rangle \ , \tag{4.13}$$

where

$$V_{\text{eff}} = Vf^2 - \beta f f'' - (2\beta/r) f f' - \beta \{ [\ln\Phi_a(r)]' + [\ln\Phi(r)]' \} f f' \ . \tag{4.14}$$

A variation without extra conditions does not work, as in the liquid phase, because we cannot find a "physically acceptable" correlation function. We therefore add an auxiliary potential or Lagrange multiplier $-\lambda$ to $V(r)$, which we hope will represent the many-body effects in the system. We write

$$I_3^s = \langle \Phi_a(r) \mid (V - \lambda) f^2 - \beta f f'' - (2\beta/r) f f' - \beta \{ [\ln\Phi_a(r)]' + [\ln\Phi(r)]' \} f f' \mid \Phi(r) \rangle \ . \tag{4.15}$$

The value of λ is determined by a variation of (4.15) with respect to f, i.e.,

$$\delta I_3^s = \delta \int_0^d dr\, r^2 \{ (V - \lambda) f^2 \Phi_a(r)\Phi(r) - \beta f f'' \Phi_a(r)\Phi(r) - (2\beta/r) f f' \Phi_a(r)\Phi(r) - \beta [\Phi_a'(r)\Phi(r) + \Phi_a(r)\Phi'(r)] f f' \} = 0 \ ,$$
$$(V - \lambda) f^2 - \beta f f' - (2\beta/r) f f' - \beta \{ [\ln\Phi_a(r)]' + [\ln\Phi(r)]' \} f f' = 0 \ , \tag{4.16}$$
$$V_{\text{eff}} - \lambda f^2 = 0 \ .$$

The expression for the effective potential V_{eff} then is

$$V_{\text{eff}} = \begin{cases} \lambda f^2 & \text{for } r \le d \ , \\ V(r) & \text{for } r > d \ . \end{cases} \tag{4.17}$$

Dividing (4.16) by f we obtain the variational equation

$$(V - \lambda) f - \beta (f'' + (2/r) f' + \{ [\ln\Phi_a(r)]' + [\ln\Phi(r)]' \} f') = 0 \ , \tag{4.18}$$

which by a proper definition of d determines λ and f self-consistently. We rearrange (4.18) and write

$$(-(\hbar^2/m)\{\nabla^2+[\nabla\ln\Phi_a(r)+\nabla\ln\Phi(r)]\cdot\nabla\}+[V(r)-\lambda])f(r)=0\ , \tag{4.19}$$

which is simplified to

$$\{-(\hbar^2/m)[\nabla^2+2\nabla\ln\Phi(r)\cdot\nabla]+[V(r)-\lambda]\}f(r)=0\ , \tag{4.20}$$

for a Boltzmann solid.

We want to solve (4.19) numerically, and we need an explicit expression for $[\ln\Phi_a(r)]'$ and $[\ln\Phi(r)]'$, i.e.,

$$[\ln\Phi_a(r)]'+[\ln\Phi(r)]'=-\nu(r+[(\nu r)^{-1}-R_{mn}/\tanh(\nu rR_{mn})]\{1-(-1)^s\nu rR_{mn}/[\sinh(\nu rR_{mn})+(-1)^s\nu rR_{mn}]\})\ . \tag{4.21}$$

The expression for I_3^s finally becomes

$$\begin{aligned}I_3^s&=\langle\Phi_a(r)\mid V_{\rm eff}\mid\Phi(r)\rangle\\&=\sqrt{\nu/2\pi}R_{mn}^{-1}\int_0^d dr\,r\lambda f^2\{\exp[-\tfrac{1}{2}\nu(r-R_{mn})^2]-\exp[-\tfrac{1}{2}\nu(r+R_{mn})^2]\}\\&\quad+\sqrt{\nu/2\pi}R_{mn}^{-1}\int_0^\infty dr\,rV(r)\{\exp[-\tfrac{1}{2}\nu(r-R_{mn})^2]-\exp[-\tfrac{1}{2}\nu(r+R_{mn})^2]\}\\&\quad+(-1)^s\{2\nu\sqrt{\nu/2\pi}\exp(-\tfrac{1}{2}\nu R_{mn}^2)\int_0^d dr\,r^2\lambda f^2\exp(-\tfrac{1}{2}\nu r^2)\\&\qquad+2\nu\sqrt{\nu/2\pi}\exp(-\tfrac{1}{2}\nu R_{mn}^2)\int_d^\infty dr\,r^2V(r)\exp(-\tfrac{1}{2}\nu r^2)\}\ ,\end{aligned} \tag{4.22}$$

which for Boltzmann statistics reduces to

$$\begin{aligned}I_3&=\sqrt{\nu/2\pi}R_{mn}^{-1}\int_0^d dr\,r\lambda f^2\{\exp[-\tfrac{1}{2}\nu(r-R_{mn})^2]-\exp[-\tfrac{1}{2}\nu(r+R_{mn})^2]\}\\&\quad+\sqrt{\nu/2\pi}R_{mn}^{-1}\int_d^\infty dr\,rV(r)\{\exp[-\tfrac{1}{2}\nu(r-R_{mn})^2]-\exp[-\tfrac{1}{2}\nu(r+R_{mn})^2]\}\ .\end{aligned} \tag{4.23}$$

To ensure a reasonable convergence of the energy expansion we have to consider the short-range correlations to be mainly two-body correlations, and we make the assumption that each particle occupies an average volume which is spherically symmetric with radius r_0, such that

$$\tfrac{4}{3}\pi r_0^3\rho=1\ . \tag{4.24}$$

The mean-square displacement of particle i from the lattice site m is given by $\phi_m(\mathbf{r}_i)$, i.e., the root-mean-square deviation is

$$\begin{aligned}R_{\rm rms}^2&=\langle\phi_m(\mathbf{r}_i)\mid(\mathbf{r}_i-\mathbf{R}_m)^2\mid\phi_m(\mathbf{r}_i)\rangle=1.5/\nu\ ,\\R_{\rm rms}&=(1.5/\nu)^{1/2}\ .\end{aligned} \tag{4.25}$$

If the range of $f(r)$, i.e., the correlations, is much longer than $2r_0-R_{\rm rms}$, more than two particles will be simultaneously correlated, and we choose our "healing" distance d to be

$$d=2r_0-R_{\rm rms}=2r_0-(1.5/\nu)^{1/2}\ . \tag{4.26}$$

The two-body contribution to the energy is finally given by (4.1), where the integrals I_1^s and I_2^s become

$$\begin{aligned}I_1^s&=-\tfrac{3}{4}\nu-\nu\left[\sqrt{\nu/2\pi}R_{mn}^{-1}\left\{\int_0^d dr\,r(1-f^2)\{[\tfrac{1}{4}\nu(r-R_{mn})^2-1]\exp[-\tfrac{1}{2}\nu(r-R_{mn})^2]\right.\right.\\&\qquad\left.\left.-[\tfrac{1}{4}\nu(r+R_{mn})^2-1]\exp[-\tfrac{1}{2}\nu(r+R_{mn})^2]\}\right\}\right]\\&\quad+(-1)^s\exp(-\tfrac{1}{2}\nu R_{mn}^2)\{-\tfrac{3}{4}\nu+\tfrac{1}{4}\nu^2R_{mn}^2-2\nu^2\sqrt{\nu/2\pi}\int_0^d dr\,r^2(1-f^2)[\tfrac{1}{4}\nu(r^2+R_{mn}^2)-\tfrac{3}{4}]\exp(-\tfrac{1}{2}\nu r^2)\}\ ,\\I_2^s&=1-\sqrt{\nu/2\pi}R_{mn}^{-1}\int_0^d dr\,r(1-f^2)\{\exp[-\tfrac{1}{2}\nu(r-R_{mn})^2]-\exp[-\tfrac{1}{2}\nu(r+R_{mn})^2]\}\\&\quad+(-1)^s\exp[-\tfrac{1}{2}\nu R_{mn}^2]\left[1-2\nu\sqrt{\nu/2\pi}\int_0^d dr\,r^2(1-f^2)\exp(-\tfrac{1}{2}\nu r^2)\right]\ ,\end{aligned} \tag{4.27}$$

which for Boltzmann statistics reduce to

$$\begin{aligned}I_1&=-\tfrac{3}{4}\nu-\nu\left[\sqrt{\nu/2\pi}R_{mn}^{-1}\left\{\int_0^d dr\,r(1-f^2)\{[\tfrac{1}{4}\nu(r-R_{mn})^2-1]\exp[-\tfrac{1}{2}\nu(r-R_{mn})^2]\right.\right.\\&\qquad\left.\left.-[\tfrac{1}{4}\nu(r+R_{mn})^2-1]\exp[-\tfrac{1}{2}\nu(r+R_{mn})^2]\}\right\}\right]\ ,\\I_2&=1-\sqrt{\nu/2\pi}R_{mn}^{-1}\int_0^d dr\,r(1-f^2)\{\exp[-\tfrac{1}{2}\nu(r-R_{mn})^2]-\exp[-\tfrac{1}{2}\nu(r+R_{mn})^2]\}\ .\end{aligned} \tag{4.28}$$

The integral I_3^s is given by (4.22), and we obtain the equation for f and λ from (4.19) and (4.21), i.e.,

$$f''=[(V-\lambda)/(\hbar^2/m)]f+[\nu(r+[(\nu r)^{-1}-R_{mn}/\tanh(\nu r R_{mn})] \times\{1-(-1)^s r\nu R_{mn}/[\sinh(\nu r R_{mn})+(-1)^s \nu r R_{mn}]\})-(2/r)]f' . \tag{4.29}$$

For Boltzmann statistics $\Phi_a(r)\to\Phi(r)$, and we get the corresponding differential equation as

$$f''=[(V-\lambda)/(\hbar^2/m)]f+(\nu\{r+[(\nu r)^{-1}-R_{mn}/\tanh(\nu r R_{mn})]\}-(2/r))f' . \tag{4.30}$$

The Lagrange parameter λ and the correlation function f are obtained self-consistently with the condition that the range of f is determined by the healing distance d which is taken from (4.26), and the boundary conditions for f are stated in (3.22). $C_2^s(ij)$ is then calculated from the integrals in (4.22) and (4.27).

The two-body contribution to the energy in the kth shell, $C_2^k(ij)$, is dependent on R_{mn} which is the distance to the kth shell, $C_2^k(ij)$ will be small for large R_{mn}, i.e., when the two particles are far apart in average, due to the short range of the interaction. This implies that it is sufficient to sum the energy contributions from the G nearest shells, where

$$|C_2^k(ij)|<\varepsilon, \quad \text{for } k=G . \tag{4.31}$$

In the numerical calculations ε is chosen to be 0.01 K. We always find $G<12$, indicating that the maximum error in the final energy due to this boundary value should be small compared to the total energy.

The expression (2.6) then is modified to

$$E/N=C_1(i)+\tfrac{1}{2}\sum_{k=1}^{G} n_k C_2^k(ij) , \tag{4.32}$$

with $C_1(i)$ given by (3.16). The energy per particle is a function of the parameter ν and must be minimized with respect to this parameter. The Boltzmann solid represents a simplification of the spin-dependent problem and the corresponding equations to be solved or calculated are then given by (4.20), (4.23), (4.28), and (4.30).

The particles must be localized in the solid phase, i.e., one particle must occupy one lattice site and have a negligible probability of occupying more than one lattice site. We may postulate that the volume occupied by the zero-point motion of the particle must be smaller than the mean available volume per particle defined by (4.24), i.e.,

$$\rho=N/\Omega=(\tfrac{4}{3}\pi r_0^3)^{-1} . \tag{4.33}$$

The volume occupied by the zero-point motion must be a function of ν which is the parameter describing the spread of the wave function $\phi_m(\mathbf{r}_i)$. Pandharipande[33] has argued that for a classical particle confined in a sphere with radius R_G, $\langle r^2\rangle$ is given by

$$\langle r^2\rangle=\tfrac{3}{5}R_G^2 , \tag{4.34}$$

and $\langle r^2\rangle$ is chosen to be $R_{\rm rms}^2$ and hence

$$R_G=(2.5/r)^{1/2} . \tag{4.35}$$

To set

$$\tfrac{4}{3}\pi R_G^3<\tfrac{4}{3}\pi r_0^3 \tag{4.36}$$

is then equivalent to defining a localization parameter

$$\Lambda=(\tfrac{4}{3}\pi r_0^3)/(\tfrac{4}{3}\pi R_G^3)=(\nu r_0^2/2.5)^{3/2} , \tag{4.37}$$

and require

$$\Lambda>1.0 . \tag{4.38}$$

We see that the parameter Λ is proportional to $\nu^{3/2}$. There are, however, two "weak" points in this procedure. The average volume occupied by the zero-point motion is determined by "classical" considerations and the probability density $|\phi_m(\mathbf{r})|^2$ is set equal to 1.0 everywhere inside the sphere with radius R_G. The quantum-mechanical expectation value of this volume is given by

$$\langle\Omega(r_i)\rangle=\langle\phi_m(\mathbf{r}_i)|\Omega(r_i)|\phi_m(\mathbf{r}_i)\rangle=\tfrac{4}{3}\pi R_\nu^3 , \quad R_\nu=(1.72/\nu)^{1/2} . \tag{4.39}$$

Also, the packing fraction is different in a bcc and a fcc (hcp) lattice, i.e., the fcc (hcp) lattice contains a greater number of particles than the bcc lattice in the same volume. This should be reflected in the lowest limit of the localization parameter $\Lambda^{\rm lim}$ such that $\Lambda_{\rm fcc}^{\rm lim}<\Lambda_{\rm bcc}^{\rm lim}$. The nearest-neighbor distance a in both crystals is given by (3.23) and (3.24), and if we require that

$$R_\nu<\tfrac{1}{2}a , \tag{4.40}$$

for a localized particle, this can be expressed as

$$\Lambda>0.84 \text{ for the bcc structure} , \quad \Lambda>0.77 \text{ for the fcc or hcp structure} . \tag{4.41}$$

V. CALCULATIONS AND RESULTS

The energy contribution from two-body correlations is now calculated by means of the modified LOCV method, i.e., we calculate the integrals and expressions (4.1), (4.22), (4.27), and (4.29), or (3.20), (4.23), (4.28), and (4.30). The total energy is then given by (2.6), i.e., by (4.32) when the original cluster expansion is truncated after the second-order term. Since the LOCV method implies a truncation of the cluster expansion keeping only one- and two-body terms, this should be compensated by the introduction of the external potential λ to represent the many-body effects and the recovery distance d defined by (4.26) to include mainly two-body correlations.

We first solve the differential equation (4.29) for a given λ, taking into account the boundary conditions (3.22). The differential equation is solved numerically by the Runge-Kutta-Nyström method, which is a general method for solving second-order differential equations,

and it is correct to fourth order in the corresponding Taylor expansion for y and y' when we have the second-order problem:

$$y''=f(x,y,y') . \tag{5.1}$$

Having some boundary conditions

$$\begin{aligned} y(x_0)&=y_0 , \\ y'(x_0)&=y_0' , \end{aligned} \tag{5.2}$$

and assuming that f has a unique solution in some interval containing x_0, we can obtain the solution by Taylor expansions for y and y'.

The calculations are done for five different potentials since the chosen two-body potential would have some influence on the results. The first one is a Lennard-Jones potential (LJ1) given by

$$V_{\mathrm{LJ1}}(r)=4\varepsilon[(\sigma_1/r)^{12}-(\sigma_1/r)^6] , \tag{5.3}$$

where

$$\begin{aligned} \varepsilon&=10.22\ \mathrm{K} , \\ \sigma_1&=2.556\ \text{Å} , \end{aligned} \tag{5.4}$$

and r is measured in angstroms. This is a semiphenomenological potential fitted by de Boer and Michels[39] to low-temperature second virial coefficients. We also try a second Lennard-Jones potential (LJ2) given by

$$V_{\mathrm{LJ2}}(r)=4\varepsilon[(\sigma_2/r)^{12}-(\sigma_2/r)^6] , \tag{5.5}$$

where

$$\sigma_2=2.62\ \text{Å} . \tag{5.6}$$

According to scattering experiments by Cavallini *et al.*,[40] the value (5.6) should be better than (5.4).

A potential given by Bruch and Mc Gee[41] is the Frost-Musulin FDD-1 potential

$$V_{\mathrm{FDD\text{-}1}}(r)=\begin{cases} -\varepsilon\{1+C[1-(r_m/r)]\}\exp\{-C[(r/r_m)-1]\} & \text{for } r\le r_2 , \\ -C_6r^{-6}-C_8r^{-8} & \text{for } r>r_2 , \end{cases} \tag{5.7}$$

where

$$\begin{aligned} &\varepsilon=12.53\ \mathrm{K},\quad C=8.008\,77 , \\ &r_m=2.98\ \text{Å},\quad C_6=10\,210\ \text{Å}^6\mathrm{K} , \\ &r_2=3.511\ \text{Å},\quad C_8=27\,670\ \text{Å}^8\mathrm{K} , \end{aligned} \tag{5.8}$$

determined by transport coefficients and second virial coefficients. Another potential is the HFDHE2 potential[42]

$$\begin{aligned} V_{\mathrm{HFDHE2}}(r)=\varepsilon\{ & A\exp(-\alpha r/r_m) \\ & -[C_6(r_m/r)^6+C_8(r_m/r)^8 \\ & +C_{10}(r_m/r)^{10}]F(r)\} , \end{aligned} \tag{5.9}$$

where

$$F(r)=\begin{cases} \exp\{-[D(r_m/r)-1]^2\} & \text{for } r/r_m\le D , \\ 1 & \text{for } r/r_m>D . \end{cases} \tag{5.10}$$

The parameters for the HFDHE2 potential are given by

$$\begin{aligned} &A=544\,850.4,\quad \varepsilon=10.8\ \mathrm{K} , \\ &\alpha=13.353\,384,\quad C_6=1.377\,324\,12 , \\ &D=1.241\,314,\quad C_8=0.425\,378\,5 , \\ &r_m=2.9673\ \text{Å},\quad C_{10}=0.1781 , \end{aligned} \tag{5.11}$$

obtained from thermal conductivities and second virial coefficients.

The last potential is the exponential-spline-Morse-Morse-spline—van der Waals (ESMMSV) potential[43] of the form

$$V_{\mathrm{ESMMSV}}(r)=\varepsilon\times\begin{cases} A\exp[-\alpha(x-1)] & \text{for } r\le 2.079\ \text{Å} , \\ \exp(a_1+(x-x_1)\{a_2+(x-x_2)[a_3+(x-x_1)a_4]\}) & \text{for } 2.079<r<2.509\ \text{Å} , \\ \exp[-2\beta(x-1)]-2\exp[-\beta(x-1)] & \text{for } 2.509\le r\le 2.97\ \text{Å} , \\ \exp[-2\beta'(x-1)]-2\exp[-\beta'(x-1)] & \text{for } 2.97<r\le 3.416\ \text{Å} , \\ b_1+(x-x_3)\{b_2+(x-x_4)[b_3+(x-x_4)b_4]\} & \text{for } 3.416<r<4.455\ \text{Å} , \\ -(C_6r^{-6}+C_8r^{-8}+C_{10}r^{-10})/\varepsilon & \text{for } r\ge 4.455\ \text{Å} , \end{cases} \tag{5.12}$$

where

$$\begin{aligned} &\varepsilon=10.57\ \mathrm{K}, && a_1=3.4469, && x_1=0.7000, \\ &x=r/r_m, && a_2=-19.0218, && x_2=0.844\,77, \\ &r_m=2.97\ \text{Å} && a_3=-28.067, && x_3=1.150\,16, \\ &\beta=6.475, && a_4=-362.002, && x_4=1.5000, \\ &\beta'=5.964, && b_1=-0.6500, && x_6=10\,140\ \text{Å}^6\mathrm{K}, \\ &A=0.343, && b_2=1.4516, && x_8=27\,380\ \text{Å}^8\mathrm{K}, \\ &\alpha=15.058, && b_3=-4.028\,89, && x_{10}=99\,230\ \text{Å}^{10}\mathrm{K}, \\ & && b_4=4.519\,27, && \end{aligned} \tag{5.13}$$

given by scattering data.[44]

VI. RESULTS FOR SOLID ^{3}He

For a system of fermions, i.e., ^{3}He atoms, we may assume that a "parallel-spin" configuration is the most favorable spin configuration in a bcc lattice. The lattice then consists of interpenetrating simple cubes, where all spins in each simple cube are parallel and the z com-

ponents of the spins in an interpenetrating cube are all antiparallel. In addition, we assume that a "mixed spin" configuration is the most favorable spin configuration in a fcc lattice. The atoms at adjacent corners of the simple cubes then have opposite z components of the spins. The face centers are also corners in other simple cubes, and one-half of the particles in a shell may have the same z component of the spin as the center particle while the other half may have a z component in the opposite direction.

If we let s be the quantum number for the total spin of two particles and M_s the projection of this spin, then

$$M_s=\begin{cases}\uparrow\downarrow=0\ , \\ \uparrow\uparrow=1\ .\end{cases} \tag{6.1}$$

If $M_s=1$ then $s=1$, and if $M_s=0$ we assume that one half of the particles are in an $s=0$ state and the other half in an $s=1$ state. This assumption gives the distribution with $\frac{1}{4}$ of the particles interacting in a singlet state and $\frac{3}{4}$ interacting in a triplet state. (See spin configurations indicated in Table I.)

For a system of ^{3}He atoms we then calculate (4.1) as

$$C_2^k(ij)=\sum_s C_2^s=\begin{cases}\frac{1}{2}[C_2^0(ij)+C_2^1(ij)] & \text{for } M_s=0\ , \\ C_2^1(ij) & \text{for } M_s=1\ ,\end{cases} \tag{6.2}$$

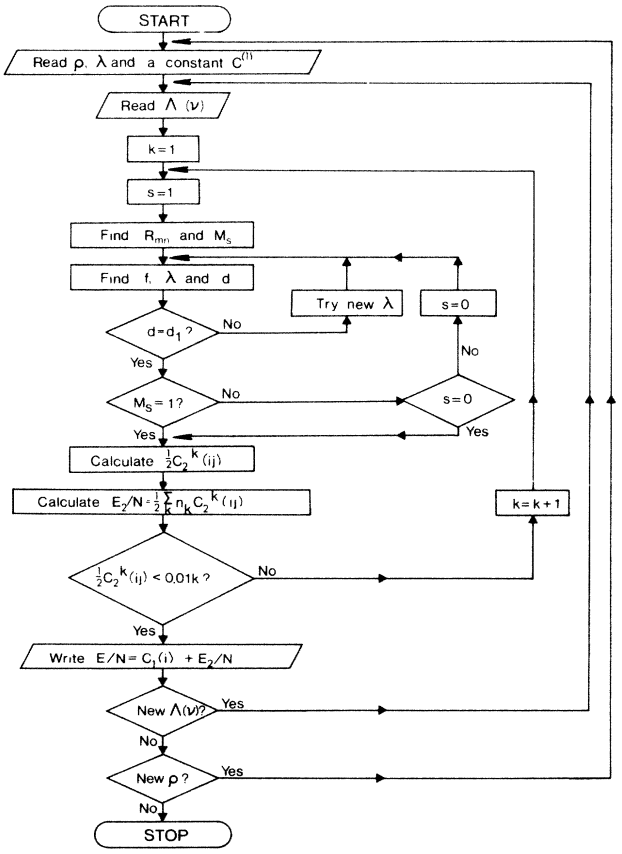

FIG. 1. The scheme of energy calculations in the LOCV method for solid ^{3}He.

for a certain crystal structure, since $\sum_s$ is to be understood as an averaged sum over s for a given M_s value. By this procedure $C_2^k(ij)$ will be an averaged two-body contribution to the energy from the kth shell. In addition, in the fcc crystal there is the possibility that one-half of the particles in a shell has the same z component of the spin as the center particle and the other half has a z component in the opposite direction. This is indicated by the symbol $\frac{1}{2}(\uparrow\uparrow+\uparrow\downarrow)$, and the two-body contribution to the energy $C_2^k(ij)$ is then given by

$$C_2^k(ij)=\sum_s C_2^s=\tfrac{1}{4}[C_2^0(ij)+3C_2^1(ij)]\ . \tag{6.3}$$

The procedure, i.e., the scheme of energy calculations by our LOCV method, is shown in Fig. 1.

For each density ρ the parameter ν in the wave function or the localization parameter Λ is determined variationally in the sense that we calculate the energy for various values of ν or Λ to obtain an optimum value for the energy for a certain value of ν. The parameter Λ is proportional to $\nu^{3/2}$ and we look for a minimum in the energy E/N with respect to Λ. (But if Λ is too small, i.e., $\Lambda<1$, the lattice structure is too diffuse and a crystal structure probably does not exist.) Energy as function of the variational parameter ν is shown in Fig. 2 for a bcc crystal and the HFDHE2 potential.

The energy contributions per shell for a bcc and a fcc lattice at a certain density for the HFDHE2 potential are shown in Tables II and III, and corresponding correlation functions $f(r)$ obtained from (4.29) are shown in Figs. 3 and 4. Total binding energy as function of density is shown in Tables IV and V, and in Figs. 5 and 6.

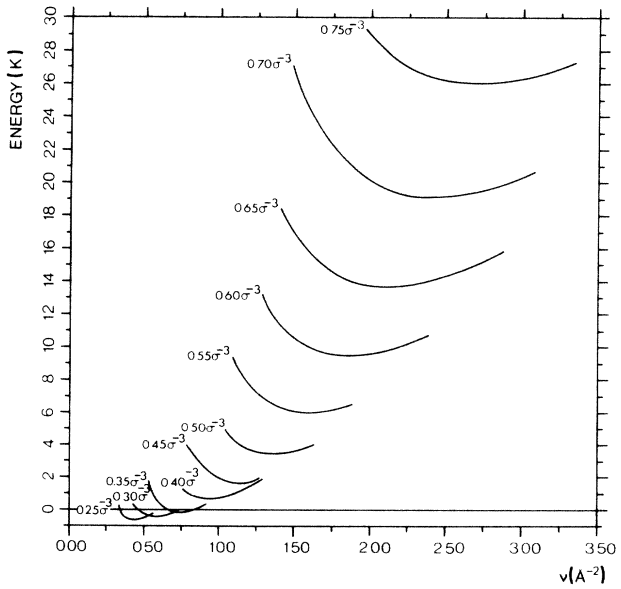

FIG. 2. Ground-state energy E/N per particle for bcc ^{3}He as function of the localization parameter ν for different densities and the HFDHE2 potential (Ref. 42). $\sigma=2.556$ Å.

TABLE II. The two-body contribution E_2/N to the energy per particle for a bcc structure with parallel spins and the HFDHE2 potential (Ref. 42). [$C_1(i)=5.38$ K and hence $E/N=-0.64$ K for $\rho=0.25\sigma^{-3}$, and $C_1(i)=32.33$ K and hence $E/N=25.99$ K for $\rho=0.75\sigma^{-3}$.] $\sigma=2.556$ Å.

ρ		R_{mn}		$\frac{1}{2}C_2^0(ij)$	$\frac{1}{2}C_2^1(ij)$	$\frac{1}{2}C_2^k(ij)$	$E_2/N=\frac{1}{2}\sum_k n_k C_2^k(ij)$
(σ^{-3})	k	(Å)	n_k	(K)	(K)	(K)	(K)
0.25	1	4.43	8	−0.2693	−0.3255	−0.2974	−2.3792
($\Lambda=1.2$)	2	5.11	6		−0.3028	−0.3028	−4.1960
	3	7.23	12		−0.0822	−0.0822	−5.1824
	4	8.48	24	−0.0267	−0.0267	−0.0267	−5.8232
	5	8.85	8		−0.0193	−0.0193	−5.9776
	6	10.22	6		−0.0068	−0.0068	−6.0184
0.75	1	3.07	8	1.7108	1.7100	1.7104	13.6832
($\Lambda=5.9$)	2	3.54	6		−1.2452	−1.2452	6.2120
	3	5.01	12		−0.4637	−0.4637	0.6476
	4	5.88	24	−0.1617	−0.1617	−0.1617	−3.2332
	5	6.14	8		−0.1215	−0.1215	−4.2052
	6	7.09	6		−0.0479	−0.0479	−4.4926
	7	7.73	24	−0.0277	−0.0277	−0.0277	−5.1574
	8	7.93	24		−0.0236	−0.0236	−5.7238
	9	8.68	24		−0.0133	−0.0133	−6.0430
	10	9.21	32	−0.0092	−0.0092	−0.0092	−6.3374

VII. RESULTS FOR SOLID ^{4}He

The calculations for solid ^{4}He become simpler than for solid ^{3}He since $s=0$ and it is not necessary to consider different spin configurations. The procedure is, otherwise, exactly the same as for solid ^{3}He, and the scheme of energy calculations by our LOCV method is shown in Fig. 7.

Total energy as function of the variational parameter ν is shown in Fig. 8, and correlation functions $f(r)$ are shown in Figs. 9 and 10. Total binding energy as function of density is shown in Table VI and VII, and in Figs. 11 and 12.

VIII. SUMMARY AND DISCUSSION

From Tables II and III we see that the two-body contribution to the energy from different shells is quite different in a bcc structure and a fcc structure. But we sum over one more shell in the bcc structure, so the difference in

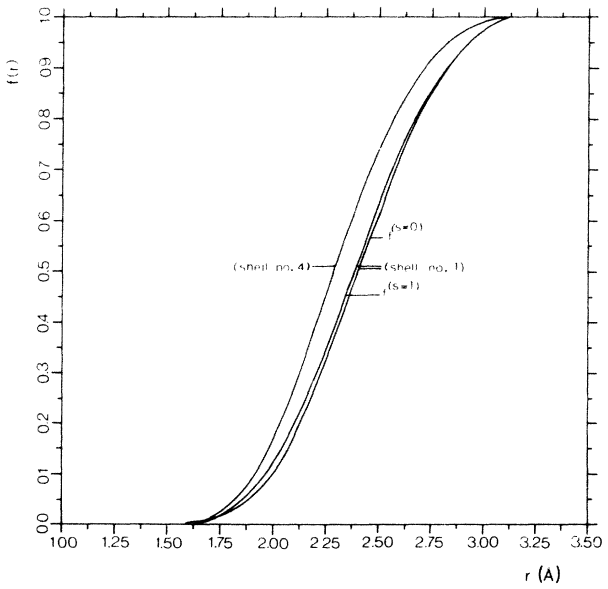

FIG. 3. Correlation functions $f(r)$ for bcc ^{3}He and the HFDHE2 potential (Ref. 42). $\rho=0.25\sigma^{-3}$. $\sigma=2.556$ Å.

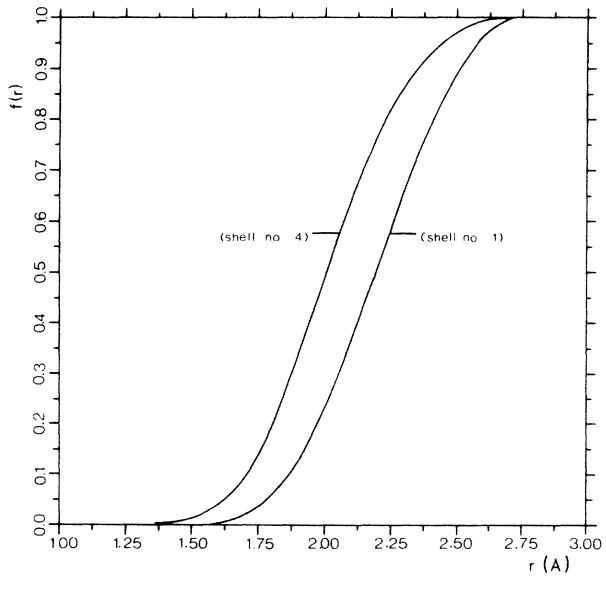

FIG. 4. Correlation functions $f(r)$ for bcc ^{3}He and the HFDHE2 potential (Ref. 42). $\rho=0.75\sigma^{-3}$. $\sigma=2.556$ Å.

TABLE III. The two-body contribution E_2/N to the energy per particle for a fcc structure with mixed spins and the HFDHE2 potential (Ref. 42). [$C_1(i)=5.38$ K and hence $E/N=-0.60$ K for $\rho=0.25\sigma^{-3}$, and $C_1(i)=32.33$ K and hence $E/N=27.14$ K for $\rho=0.75\sigma^{-3}$.] $\sigma=2.556$ Å.

ρ (σ^{-3})	k	R_{mn} (Å)	n_k	$\frac{1}{2}C_2^0(ij)$ (K)	$\frac{1}{2}C_2^1(ij)$ (K)	$\frac{1}{2}C_2^k(ij)$ (K)	$E_2/N=\frac{1}{2}\sum_k n_k C_2^k(ij)$ (K)
0.25	1	4.55	12	−0.3350	−0.2873	−0.2992	−3.5907
($\Lambda=1.2$)	2	6.44	6	−0.1585	−0.1572	−0.1579	−4.5381
	3	7.89	24	−0.0454	−0.0453	−0.0453	−5.6253
	4	9.11	12		−0.0157	−0.0157	−5.8137
	5	10.18	24	−0.0070	−0.0070	−0.0070	−5.9817
0.75	1	3.16	12	0.8698	0.8702	0.8701	10.4412
($\Lambda=5.9$)	2	4.47	6	−0.9359	−0.9359	−0.9359	4.8258
	3	5.47	24	−0.2606	−0.2606	−0.2606	−1.4286
	4	6.32	12		−0.1010	−0.1010	−2.6406
	5	7.06	24	−0.0491	−0.0491	−0.0491	−3.8190
	6	7.74	8	−0.0275	−0.0275	−0.0275	−4.0390
	7	8.36	48	−0.0169	−0.0169	−0.0169	−4.8502
	8	8.93	6		−0.0112	−0.0112	−4.9174
	9	9.47	36	−0.0077	−0.0077	−0.0077	−5.1946

the R_{mn} for the last shell and in total energy becomes quite small.

From Figs. 2 and 8 we see that the ground-state energy does not depend too strongly on the parameter ν or Λ. The chosen Λ, however, depends rather strongly on the particle density or the molar volume. It increases as the volume decreases, corresponding to increasing localization of the particles with increasing density. At higher pressures the displacement of the atoms from their equilibrium positions is reduced, and there should be less penetration of the wave function into the strongly repulsive part of the potential. This, however, is compensated by the fact that the atoms now are close together, and the ground-state energy actually becomes more repulsive with increasing density as seen in Tables IV–VII and in Figs. 5, 6, 11, and 12.

Since the calculated energy of solid helium depends rather sensitively on the choice of two-body potential, it is difficult to use our results to justify the methods being used and the approximations involved. Only two-body correlations are, in principle, included in the calculations, and a small change in the potential can produce a large change in the calculated ground-state energy because of a rather delicate balance between kinetic and potential energy. We see that for solid ^{3}He the ESMMSV potential gives approximately 1 K less binding than the FDD-1 potential for a density $\rho=0.25\sigma^{-3}$, and the ESMMSV potential gives approximately 7 K less binding than the LJ1 potential. Some of our results are, however, very close to experimental results as seen in Figs. 5, 6, 11, and 12.

For solid ^{3}He, the calculated results for the binding energy vary from −1.25 K for the FDD-1 potential to −0.23 K for the ESMMSV potential at a density $\rho=0.25\sigma^{-3}$. For $\rho=0.75\sigma^{-3}$, the calculated results vary from 22.77 K for the LJ1 potential to 29.69 K for the ESMMSV potential. For solid ^{4}He, the calculated results for the binding energy vary from −5.01 K for the FDD-1 potential to −3.96 K for the LJ1 potential at a density

TABLE IV. Energy per particle E/N for solid ^{3}He as function of particle density ρ for the FDD-1 potential (Ref. 41).

	bcc			fcc		
$\rho(\sigma^{-3})$	Λ	ν (Å^{-2})	E/N (K)	Λ	ν (Å^{-2})	E/N (K)
0.25	1.2	0.45	−1.25	1.2	0.45	−1.21
0.30	1.5	0.58	−1.28	1.6	0.61	−1.24
0.35	1.9	0.76	−1.19	1.9	0.76	−1.08
0.40	2.3	0.94	−0.60	2.3	0.94	−0.46
0.45	2.8	1.16	0.25	2.8	1.16	0.33
0.50	3.3	1.39	1.73	3.3	1.39	2.01
0.55	3.8	1.63	4.06	3.8	1.63	4.46
0.60	4.5	1.93	7.28	4.5	1.93	7.78
0.65	5.1	2.21	11.32	5.0	2.18	12.22
0.70	5.7	2.50	16.74	5.5	2.44	17.91
0.75	6.4	2.83	23.54	6.3	2.80	24.72

TABLE V. Energy per particle E/N for solid ^{3}He as function of particle density ρ for the ESMMSV potential (Ref. 43).

	bcc			fcc		
$\rho(\sigma^{-3})$	Λ	ν (Å^{-2})	E/N (K)	Λ	ν (Å^{-2})	E/N (K)
0.25	1.2	0.45	−0.23	1.3	0.47	−0.09
0.30	1.5	0.58	0.02	1.6	0.61	0.13
0.35	1.9	0.76	0.42	2.0	0.78	0.62
0.40	2.4	0.97	1.37	2.3	0.94	1.57
0.45	2.7	1.13	2.63	2.7	1.13	2.78
0.50	3.2	1.36	4.52	3.2	1.36	4.58
0.55	3.7	1.60	7.32	3.7	1.60	7.74
0.60	4.3	1.87	11.01	4.3	1.87	11.54
0.65	4.8	2.12	15.50	4.8	2.12	16.42
0.70	5.4	2.41	21.36	5.4	2.41	22.52
0.75	6.1	2.74	28.53	6.1	2.74	29.69

TABLE VI. Total energy per particle E/N for solid ^{4}He as function of particle density ρ for the FDD-1 potential (Ref. 41). $\sigma=2.556$ Å.

	bcc			fcc			hcp		
$\rho(\sigma^{-3})$	Λ	ν (Å^{-2})	E/N (K)	Λ	ν (Å^{-2})	E/N (K)	Λ	ν (Å^{-2})	E/N (K)
0.30	1.5	0.58	−5.01	1.5	0.58	−5.06	1.5	0.58	−4.99
0.35	1.9	0.76	−5.74	1.9	0.76	−5.69	1.9	0.76	−5.64
0.40	2.4	0.97	−6.13	2.4	0.97	−6.03	2.4	0.97	−6.03
0.45	3.0	1.21	−6.38	3.1	1.24	−6.31	3.1	1.24	−6.06
0.50	3.6	1.47	−6.14	3.6	1.47	−5.87	3.6	1.47	−5.67
0.55	4.3	1.77	−5.18	4.3	1.77	−4.80	4.3	1.77	−4.78
0.60	5.1	2.10	−3.46	5.1	2.10	−2.97	5.1	2.10	−2.98
0.65	5.8	2.41	−1.06	5.8	2.41	−0.20	5.8	2.41	−0.25
0.70	6.6	2.76	2.63	6.6	2.76	3.75	6.6	2.76	3.69
0.75	7.4	3.12	7.57	7.4	3.12	8.71	7.4	3.12	8.92

TABLE VII. Total energy per particle E/N for solid ^{4}He as function of particle density ρ for the ESMMSV potential (Ref. 43). $\sigma=2.556$ Å.

	bcc			fcc			hcp		
$\rho(\sigma^{-3})$	Λ	ν (Å^{-2})	E/N (K)	Λ	ν (Å^{-2})	E/N (K)	Λ	ν (Å^{-2})	E/N (K)
0.30	1.4	0.56	−3.96	1.4	0.56	−4.02	1.4	0.56	−3.95
0.35	1.8	0.73	−4.30	1.8	0.73	−4.24	1.8	0.73	−4.19
0.40	2.3	0.94	−4.23	2.3	0.94	−4.13	2.3	0.94	−4.12
0.45	2.9	1.19	−4.01	2.9	1.19	−3.93	2.9	1.19	−3.67
0.50	3.4	1.42	−3.29	3.4	1.42	−3.04	3.4	1.42	−2.82
0.55	4.1	1.71	−1.81	4.1	1.71	−1.47	4.1	1.71	−1.93
0.60	4.8	2.01	0.40	4.8	2.01	0.86	4.8	2.01	0.95
0.65	5.4	2.30	3.32	5.4	2.30	4.14	5.4	2.30	4.24
0.70	6.1	2.62	7.48	6.1	2.62	8.53	6.1	2.62	8.65
0.75	6.6	2.89	12.86	6.7	2.92	13.90	6.7	2.92	14.11

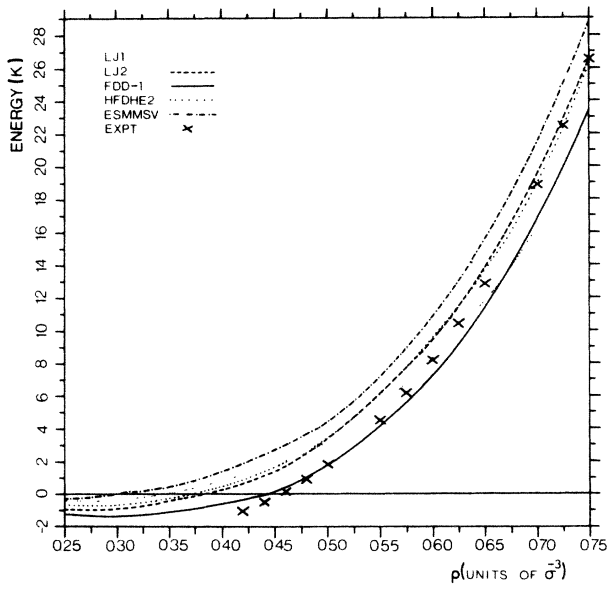

FIG. 5. Ground-state energy E/N per particle for bcc ^{3}He as function of particle density ρ for different potentials. $\sigma=2.556$ Å.

$\rho=0.30\sigma^{-3}$. For $\rho=0.75\sigma^{-3}$ the calculated results vary from 7.22 K for the LJ1 potential to 12.86 K for the ESMMSV potential. From Figs. 5 and 11 we see that the FDD-1 potential gives energies very close to experimental values for low densities, and the LJ2 and the HFDHE2 potentials give energies very close to experimental values for high densities. The ESMMSV potential, which should be the most modern potential, seems to give too little

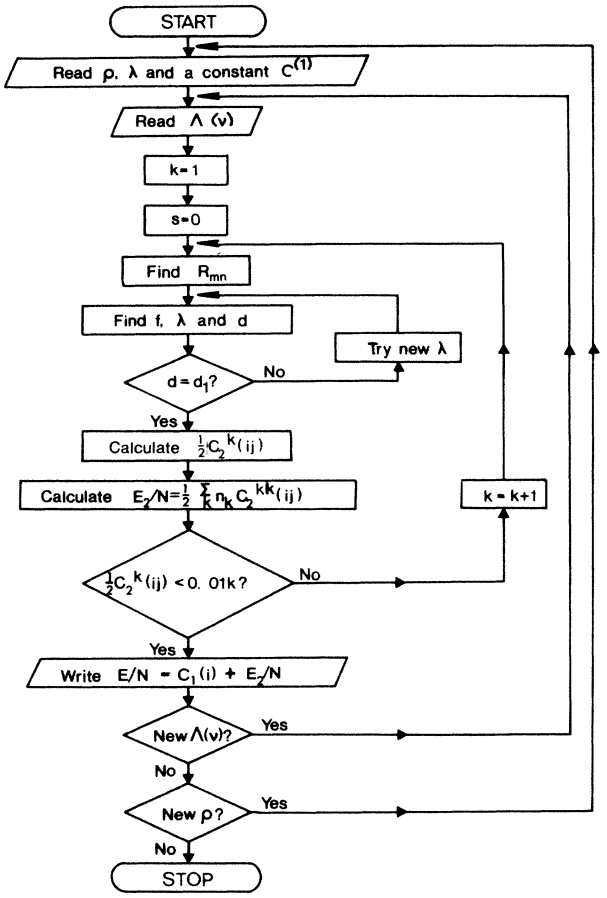

FIG. 7. The scheme of energy calculations in the LOCV method for solid ^{4}He.

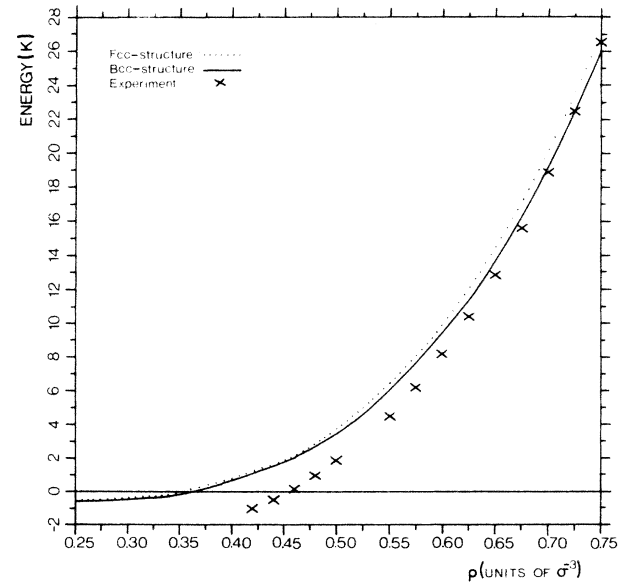

FIG. 6. Ground-state energy E/N per particle for bcc and fcc ^{3}He as function of particle density ρ for the HFDHE2 potential (Ref. 42). $\sigma=2.556$ Å.

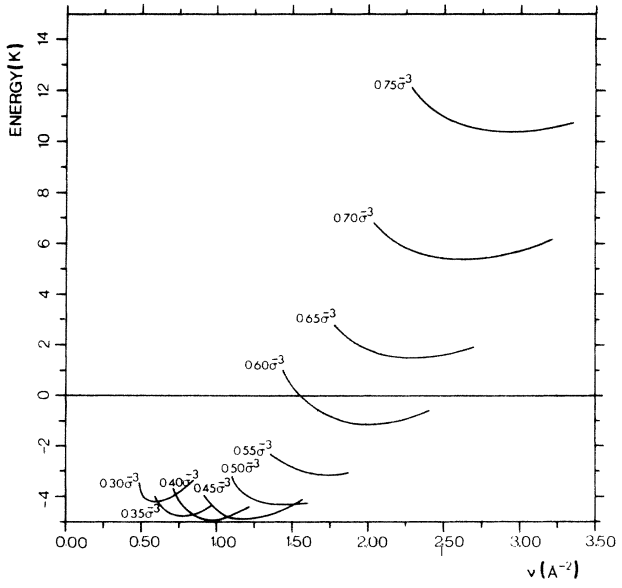

FIG. 8. Ground-state energy E/N per particle for bcc ^{4}He as function of the localization parameter ν for different densities and the HFDHE2 potential (Ref. 42). $\sigma=2.556$ Å.

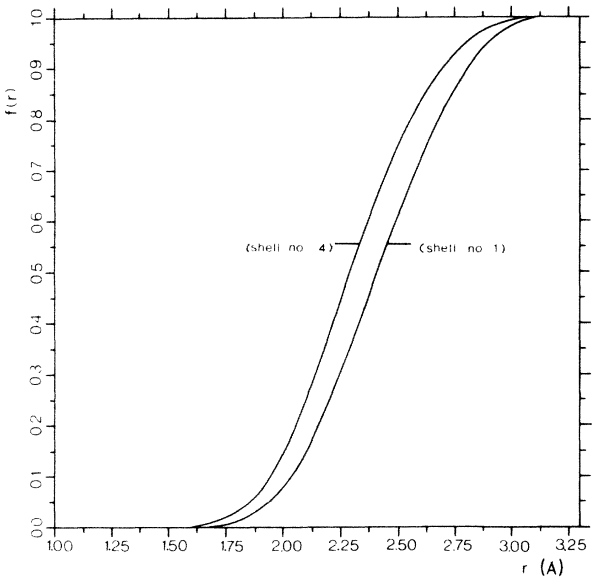

FIG. 9. Correlation functions $f(r)$ for bcc ^{4}He and the HFDHE2 potential (Ref. 42). $\rho=0.30\sigma^{-3}$. $\sigma=2.556$ Å.

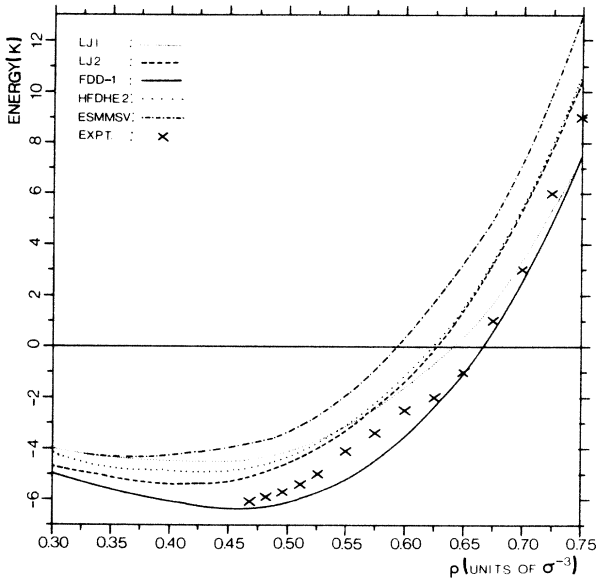

FIG. 11. Ground-state energy E/N per particle for bcc ^{4}He as function of particle density ρ for different potentials. $\sigma=2.556$ Å.

binding energy at all densities for both solid ^{3}He and ^{4}He, but it is possibly the best all-around potential since the missing binding energy could be due to our LOCV method.

The healing distance (4.26) is given by

$$d=2.0r_n-(1.5/\nu)^{1/2}\,,$$
$$r_n=(3/4\pi\rho[\sigma^{-3}])^{1/3}\sigma\,, \tag{8.1}$$
$$\sigma=2.556\text{ Å}\,.$$

The localization parameter Λ or ν will increase with increasing density. The term $2r_n$ will, however, decrease faster than the term $(1.5\nu)^{1/2}$ so the healing distance d will also decrease with increasing density, as can be seen from Figs. 3, 4, 9, and 10. We also see that we get decreasing healing distance with increasing shell number for a certain density.

From Tables IV–VII we see that we get most binding energy for the bcc structure, and less binding for the fcc (hcp) structure. The energy difference between the structures is, however, always rather small, varying from approximately 0.1 K at low densities to approximately 1 K

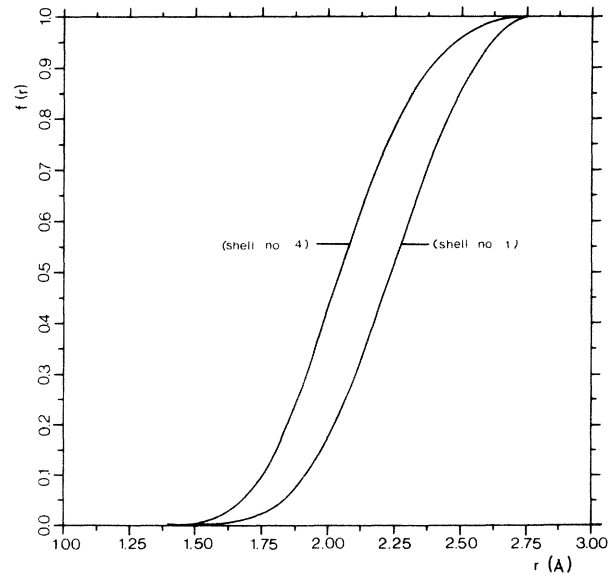

FIG. 10. Correlation functions $f(r)$ for bcc ^{4}He and the HFDHE2 potential (Ref. 42). $\rho=0.75\sigma^{-3}$. $\sigma=2.556$ Å.

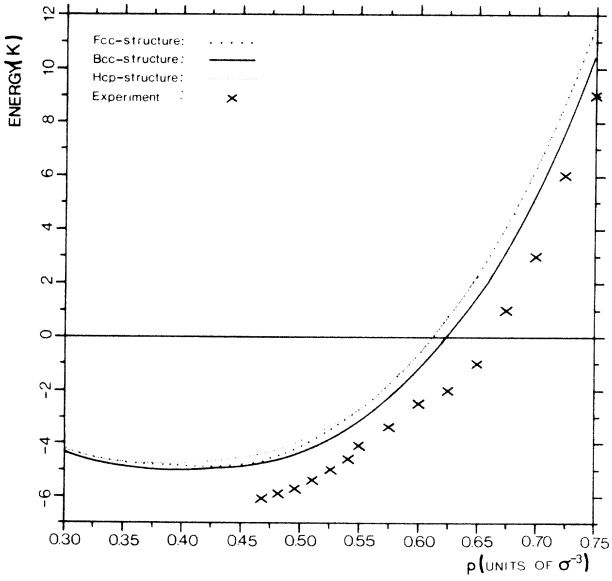

FIG. 12. Ground-state energy E/N per particle for bcc, fcc, and hcp ^{4}He as function of particle density ρ for the HFDHE2 potential (Ref. 42). $\sigma=2.556$ Å.

at high densities.

For each density ρ the parameter ν in our calculations or the localization parameter Λ is determined variationally in the sense that we calculate the energy for various values of ν or Λ to obtain an optimum value for the energy for a certain value of ν. Other earlier[21] calculations have given larger values for ν corresponding to stronger localization, i.e., 1.1 to 1.4 Å^{-2} instead of our values $\nu \approx 1.0$ Å^{-2} for solid ^{3}He at a particle density of $0.42\sigma^{-3}$ or a molar volume of 24 cm^3/mole, and 1.8 to 2.2 Å^{-2} instead of our values $\nu \approx 1.5$ Å^{-2} for solid ^{4}He at a particle density of $0.50\sigma^{-3}$ or a molar volume of 20 cm^3/mol. For higher densities, we get corresponding differences, i.e., earlier calculations[21] give values for ν of 2.0 to 2.4 Å^{-2} instead of our values $\nu \approx 1.7$ Å^{-2} for solid ^{3}He at a particle density of $0.56\sigma^{-3}$ or a molar volume of 18 cm^3/mol, and 3.4 to 4.3 Å^{-2} instead of our values $\nu \approx 2.9$ Å^{-2} for solid ^{4}He at a particle density of $0.72\sigma^{-3}$ or a molar volume of 14 cm^3/mol.

Our theoretical results for the ground-state energy per particle are -0.3 to $+1.8$ K for solid ^{3}He at a particle density of $0.42\sigma^{-3}$ or a molar volume of 24 cm^3/mol, and -6.1 to -3.2 K for solid ^{4}He at a particle density of $0.50\sigma^{-3}$ or a molar volume of 20 cm^3/mol. Corresponding Monte Carlo calculations[29,31] give $+0.7$ to $+0.9$ K for ^{3}He and -4.7 to -4.2 K for ^{4}He, while the corresponding experimental results are -1.0 and -5.6 K, respectively. For higher densities, we obtain similarly ground-state energies per particle of $+4.6$ to $+8.0$ K for solid ^{3}He at a particle density of $0.56\sigma^{-3}$ or a molar volume of 18 cm^3/mol, and $+4.4$ to $+9.4$ K for solid ^{4}He at a particle density of $0.72\sigma^{-3}$ or a molar volume of 14 cm^3/mol. Corresponding Monte Carlo calculations[29,31] give $+5.1$ to $+6.4$ K for ^{3}He and $+5.6$ to $+6.6$ K for ^{4}He, while corresponding experimental results are $+5.1$ and $+5.2$ K, respectively.

[1]G. Leibfried and W. Ludwig, in *Solid State Physics,* edited by H. Ehrenreich, F. Seitz, and D. Turnbull (Academic, New York, 1961), Vol. 12, p. 275.

[2]D. J. Hooton, Philos. Mag. **46**, 422 (1955); **46**, 433 (1955); **46**, 485 (1955); **46**, 701 (1955); **3**, 49 (1958).

[3]R. P. Hurst and J. M. H. Levelt, J. Chem. Phys. **34**, 54 (1961).

[4]N. Bernardes and H. Primakoff, Phys. Rev. Lett. **2**, 290 (1959); **3**, 144 (1959); Phys. Rev. **119**, 968 (1960).

[5]N. Bernardes, Phys. Rev. **120**, 1927 (1969).

[6]E. M. Saunders, Phys. Rev. **126**, 1724 (1962).

[7]R. Jastrow, Phys. Rev. **98**, 1479 (1955).

[8]R. L. Garwin and A. Landesman, Physics **2**, 107 (1965).

[9]N. G. Van Kampen, Physica **27**, 783 (1961).

[10]L. H. Nosanow and G. L. Shaw, Phys. Rev. **128**, 546 (1962).

[11]L. H. Nosanow, Phys. Rev. Lett. **13**, 270 (1964); Phys. Rev. **146**, 120 (1966).

[12]J. H. Hetherington, W. J. Mullin, and L. H. Nosanow, Phys. Rev. **154**, 175 (1967).

[13]W. J. Mullin, L. H. Nosanow, and P. M. Steinback, Phys. Rev. **188**, 140 (1969).

[14]K. A. Brueckner and J. Frohberg, Prog. Theor. Phys. Suppl. (1965), p. 383.

[15]K. A. Brueckner and R. Thieberger, Phys. Rev. **178**, 362 (1969).

[16]S. B. Trickey, Phys. Rev. **166**, 177 (1968).

[17]W. E. Massey and C.-W. Woo, Phys. Rev. **169**, 241 (1969).

[18]C.-W. Woo and W. E. Massey, Phys. Rev. **177**, 272 (1969).

[19]F. Iwamoto and H. Namaizawa, Prog. Theor. Phys. Suppl. **37**, 234 (1966); **45**, 682 (1971).

[20]B. H. Brandow, Ann. Phys. (N.Y.) **74**, 112 (1971).

[21]E. Østgaard, J. Low Temp. Phys. **5**, 237 (1971); Physica **74**, 113 (1974).

[22]K. A. Brueckner and J. L. Gammel, Phys. Rev. **105**, 1679 (1957); **109**, 1023 (1958).

[23]H. A. Bethe and J. Goldstone, Proc. R. Soc. London, Ser. A **238**, 551 (1957).

[24]R. A. Guyer, Solid State Commun. **7**, 315 (1969).

[25]R. A. Guyer and L. I. Zane, Phys. Rev. **188**, 445 (1969).

[26]H. R. Glyde and F. C. Khanna, Can. J. Phys. **49**, 2997 (1971).

[27]H. Horner, Phys. Rev. A **1**, 1722 (1970).

[28]C. Ebner and C. C. Sung, Phys. Rev. A **4**, 269 (1971).

[29]J.-P. Hansen and D. Levesque, Phys. Rev. **165**, 293 (1968).

[30]J.-P. Hansen, Phys. Lett. **30A**, 214 (1969); **34A**, 25 (1971).

[31]J.-P. Hansen and E. L. Pollock, Phys. Rev. A **5**, 2651 (1972).

[32]D. M. Ceperley, G. V. Chester, M. H. Kalos, and P. A. Whitlock, J. Phys. (Paris) Colloq. **39**, C6-1298 (1978).

[33]V. R. Pandharipande, Nucl. Phys. **A217**, 1 (1973).

[34]R. Mittet and E. Østgaard, Nucl. Phys. **A411**, 417 (1983).

[35]V. R. Pandharipande, Nucl. Phys. **A174**, 641 (1971); **A178**, 123 (1971).

[36]V. R. Pandharipande and H. A. Bethe, Phys. Rev. C **4**, 1312 (1973).

[37]E. Lunnan and E. Østgaard, Physica **101B**, 22 (1980).

[38]O. Forseth and E. Østgaard, Phys. Scr. **24**, 519 (1981).

[39]J. de Boer and A. Michels, Physica **5**, 945 (1938).

[40]M. Cavallini, L. Meneyhetti, G. Scoles, and M. Yealhand, Phys. Rev. Lett. **24**, 1469 (1970).

[41]L. W. Bruch and I. J. McGee, J. Chem. Phys. **46**, 2959 (1967); **52**, 5889 (1971).

[42]R. A. Aziz, V. P. S. Nain, J. S. Carley, W. L. Taylor, and G. T. McConville, J. Chem. Phys. **70**, 4330 (1979).

[43]A. L. J. Burgmans, J. M. Farrar, and Y. T. Lee, J. Chem. Phys. **54**, 1345 (1976).

[44]R. Feltgen, H. Pauly, F. Torello, and H. Vehmeyer, Phys. Rev. Lett. **30**, 820 (1973).